

# Design Method and Mechanism Study of LDMOS to Conquer Stress Induced Degradation of Leakage Current and HTRB Reliability

Kanako Komatsu, Tomoko Kinoshita, Saori Shioda, Toshihiro Sakamoto, Koji Kimura, Koji Yonemura and Fumitomo Matsuoka  
 Toshiba Electronic Devices & Storage Corporation  
 580-1 Horikawa-cho, Saiwai-ku, Kawasaki-city, Kanagawa  
 212-8520, Japan  
 E-mail: kanako.komatsu@toshiba.co.jp

Keita Takahashi, Akihiro Urata, Shoichi Sakaguchi and Takahito Nagamatsu  
 Japan Semiconductor Corporation Oita Operations  
 3500 Oaza Matsuoka, Oita-city, Oita  
 870-0197, Japan  
 E-mail: keita2.takahashi@toshiba.co.jp

**Abstract**—8V NchLDMOS, which has an enough tolerance against both a leakage current ( $I_{dss}$ ) increase and high temperature reverse bias (HTRB) degradation is proposed. Dislocation growth, which results in  $I_{dss}$  increase and has a negative influence on HTRB reliability, occurs because of a high-dose ion implantation and/or mechanical stress due to shallow trench isolation (STI). The studied 8V NchLDMOS was developed by taking into account the mechanism understanding to prevent the dislocation growth affecting the device characteristics, and as a result, achieved a competitive low resistance ( $R_{onA}=1.67m\Omega\cdot mm^2$ ).

**Keywords**—LDMOS, dislocation growth, leakage current, high temperature reverse bias

## I. INTRODUCTION

LDMOS is widely used for Mixed-signal ICs. In case of using for output devices, LDMOS's size, which has a considerable impact on the total chip size, is an important factor. Therefore, low on-resistance ( $R_{on}$ ) is an indispensable characteristics of LDMOS [1-5]. At the same time, keeping the LDMOS's  $I_{dss}$  low is also significant in order to realize a low stand-by power. Moreover,  $I_{dss}$  increase during the product operation leads to circuit operation failure and IC's lifetime degradation. A number of studies have been done to design a low- $I_{dss}$  device [6] with obtaining a high yield [7] and also to suppress  $I_{dss}$  increase from the reliability viewpoint [8-9]. In this study, we focus on the relation between device characteristics and the impact of the mechanical stress due to STI, and propose the device design which is tolerate against both  $I_{dss}$  increase and high HTRB degradation with keeping a low  $R_{on}$ .

## II. DEVICE STRUCTURES AND EXPERIMENT

The device was fabricated using 0.13  $\mu m$  CMOS-DMOS technology [8]. Plane and cross-sectional schematic views of conventional 8V NchLDMOS are shown in Fig.1. In the evaluated device, the channel length is 0.3  $\mu m$  and the gate oxide thickness is 12.5 nm. The off-state drain-source breakdown voltage ( $BV_{dss}$ ) is 10 V, which can ensure 8 V operation considering  $BV_{dss}$  variance and temperature dependence. The source and the backgate electrodes were shorted by layout design. STI is located only at the outer region of the device. In this study, two kinds of STI filling materials were studied, since STI filling material remains in

the device structure, that it has a great influence on the device characteristics, yield, and reliability. Material-A is deposited by a method of a high density plasma assisted chemical vapor deposition (CVD) processing and material-B is deposited by an atmospheric pressure CVD processing.

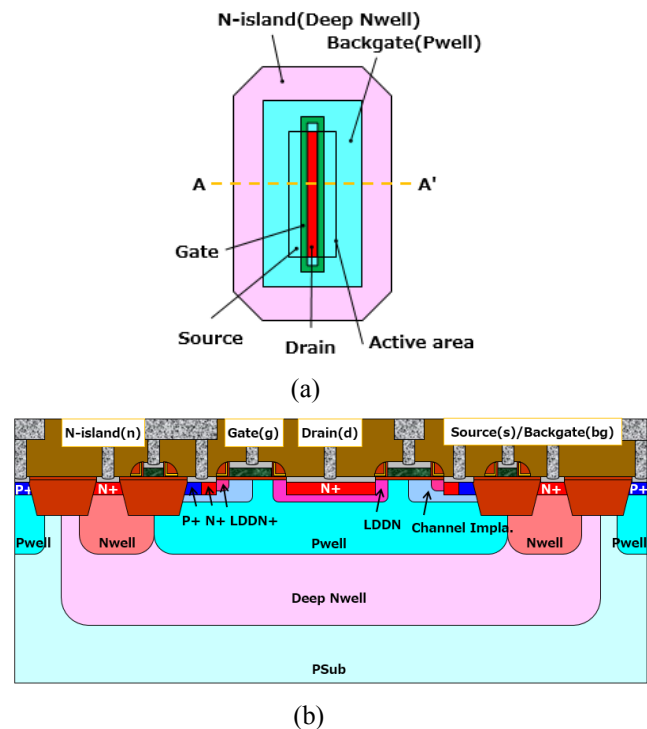


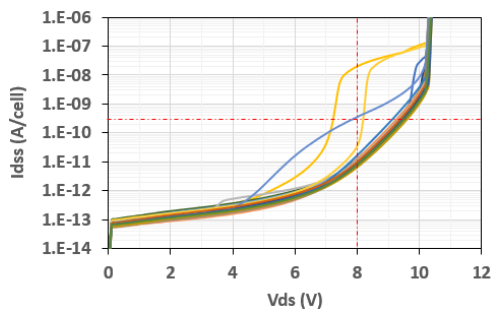
Fig. 1: (a) Plane and (b) cross-sectional views (A-A') of a conventional 8V NchLDMOS structure.

## III. RESULTS AND DISCUSSIONS

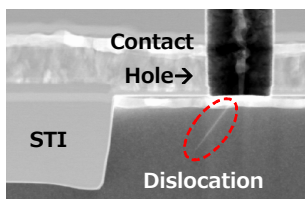
### A. Initial leakage current

$I_d$ - $V_d$  curves of the conventional structure which applied material-A as a STI filling material (Fig. 2(a)) show that some of the chips have  $I_{dss}$  which exceeds 3pA/cell below  $V_{ds}=8V$ . Fig. 2(b) is a TEM image of the fail chip. The dislocation was observed under the contact hole near the STI. A high-dose ion implantation forms an amorphous Si layer. The annealing follows to activate the amorphous Si layer, and during a recrystallization, the Si is activated under the

high stress due to the STI filling material, which has a different thermal expansion coefficient compared to Si. While the recrystallization carries on, the value of STI induced stress which affects the Si might exceed a critical stress, which results in the dislocation formation. We assume that the origin of the dislocation might be the high-dose ion implantation damage combined with STI stress, and thus, we investigated an influence of high-dose ion implantation damage on the  $I_{dss}$  failure rate and the Ron (Fig. 3). As the phosphorus dose decreases, the defect generation decreases. However, decreasing the phosphorus dose results in the Ron increase simultaneously, thus this approach is not preferable for LDMOS performance. Although applying a thermal process for a long time to recover the Si damage caused by high-dose ion-implantation is not suitable for a shrunk process because of a design restriction. Meanwhile, we also studied two kinds of STI filling material having different stress against Si, material-A shows higher stress during annealing than material-B, and stress value are dependent on their film density. In the case of applying the material-B, no  $I_{dss}$  fail chip was observed even at  $4.6 \times 10^{15} \text{ cm}^{-2}$  dose condition (Fig. 4), although some fail chips were observed at the same dose condition in the case of material-A (Fig. 2(a)).



(a)



(b)

Fig. 2: (a)  $I_{dss}$ - $V_{ds}$  curves ( $V_{gs}=0V$ ,  $T=27^\circ C$ ) of conventional structure with STI filling material-A at  $4.6 \times 10^{15} \text{ cm}^{-2}$  dose condition (b) cross-sectional TEM image of the fail chip.

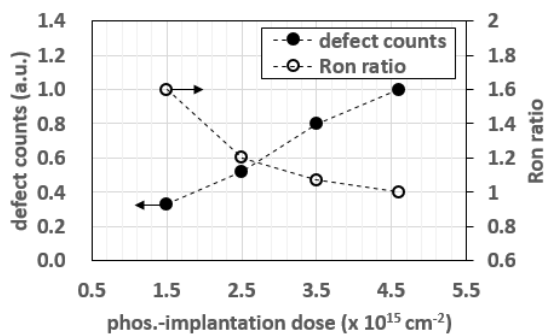


Fig. 3: Dependence of the  $I_{dss}$  failure rate and the Ron of conventional structure with STI filling material-A on Phos. dose. \*3200cell array pattern of 8V NchLDMOS

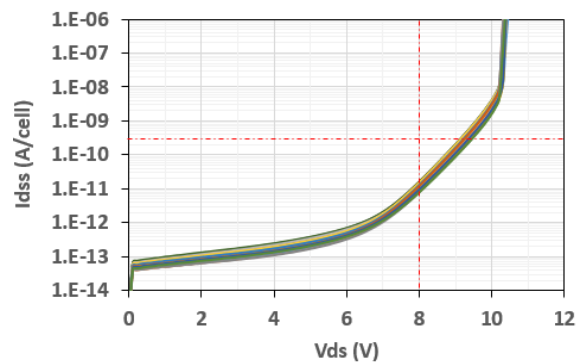
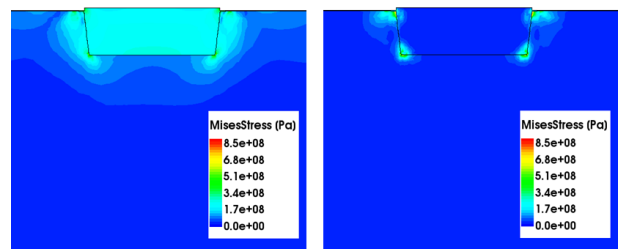


Fig. 4:  $I_{dss}$ - $V_{ds}$  curves ( $V_{gs}=0V$ ,  $T=27^\circ C$ ) of conventional structure with STI filling material-B at  $4.6 \times 10^{15} \text{ cm}^{-2}$  dose condition.



(a)

(b)

Fig. 5: Simulation results of Mises stress applying (a) material-A and (b) material-B as a STI filling material. Applied stress is -300MPa and 0MPa, respectively.

To evaluate the stress difference between material-A and B, a process simulation was carried out based on the estimated stress value, -300MPa in material-A and 0MPa in material-B, respectively. These values were calculated from the warp evaluation on bare wafers [9]. Fig. 5 shows a calculated stress distribution during the densification under the high temperature annealing which has a strong relation to the dislocation growth. In the case of material-A, higher stress value is observed at the Si substrate near a STI, and it is suppressed in material-B case. This high stress prevents the recrystallization of the Si, thus leaves the dislocation. The simulated results well describe the  $I_{dss}$ - $V_{ds}$  characteristics difference between material-A and B (Fig. 2(a) and Fig. 4).

### B. High temperature reverse bias (HTRB)

We assume that this  $I_{dss}$  failure rate difference occurs from dislocation growth rate related to Si stress from STI filling materials. HTRB test was also carried out to evaluate the influence of STI stress. The  $I_{dss}$  continuously increased under the HTRB stress for both material-A and B (Fig. 6). The results indicate that reducing the stress from the STI filling material is not enough to ensure the reliability. Further approach is needed to prevent the  $I_{dss}$  increase under the HTRB stress. The HTRB degradation could be caused by the trapped charge at STI/Si-interface [10], in that case, the trapped charge is de-trapped by applying wafer baking after HTRB test, which leads to  $I_{dss}$  increase suppression. However, the result of wafer baking showed  $I_{dss}$  increase (Fig. 7). The result is unreasonable with the assumption, and thus we propose another mechanism to explain this phenomenon.

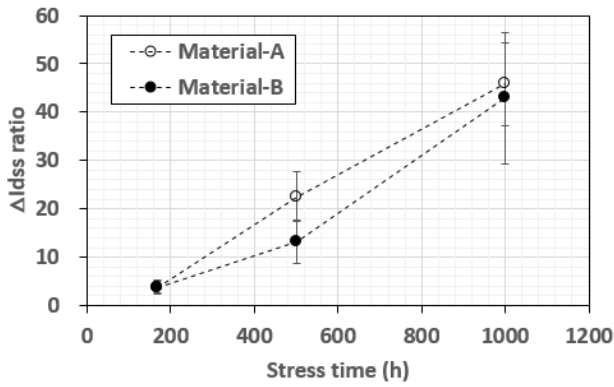


Fig. 6: Measured  $I_{dss}/I_{dss0}$  ( $V_{ds}=8V$ ,  $V_{gs}=0V$ ,  $T=27^\circ C$ , 8 points) under the HTRB stress ( $V_{ds}=8V$ ,  $V_{gs}=0V$ ,  $T=150^\circ C$ ) of conventional structure with STI filling material-A and B.

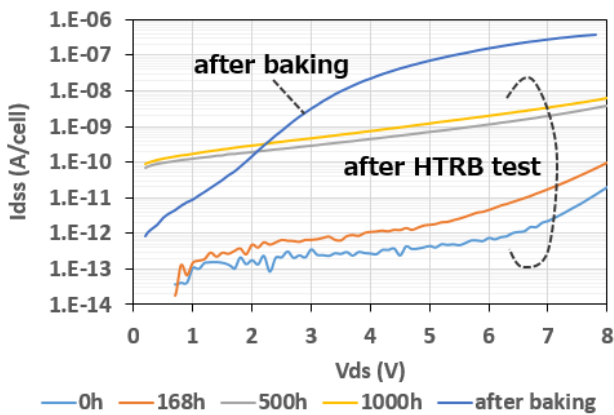


Fig. 7: Measured  $I_{dss}$ - $V_{ds}$  ( $V_{gs}=0V$ ,  $T=27^\circ C$ ) of conventional structure with STI filling material-A under the HTRB stress ( $V_{ds}=8V$ ,  $V_{gs}=0V$ ,  $T=150^\circ C$ ) and after wafer baking for 24h at  $250^\circ C$ .

#### IV. MECHANISM OF $I_{dss}$ INCREASE UNDER THE HTRB STRESS

Fig. 8 shows the explanation of the mechanism of  $I_{dss}$  increase under the HTRB stress.  $I_{dss}$  increase after HTRB is considered to relate to both  $H^+$  termination to a dislocation and de-termination from the dislocation. Firstly, the dislocation due to high-dose implantation near the STI/Si edge grows. Secondly, the dislocation is treated by hydrogen ( $H^+$ ) termination to the dangling bond under the  $N_2/H_2$  anneal. This is because the  $I_{dss}$  at 0s show low  $I_{dss}$  (Fig.7). In spite of this  $H^+$  termination during  $N_2/H_2$  anneal,  $H^+$  de-terminates from the dangling bond under the HTRB stress. As a result, the leakage current after the HTRB stress increases. From this assumption, the cause of the  $I_{dss}$  increase under the HTRB stress is as same as the  $I_{dss}$  failure rate increase due to a dislocation growth. In order to prevent the dislocation growth, the first approach is to select a preferable STI filling material, which to suppress a stress inside the Si less than its critical stress. However, just modifying the STI filling material was not enough to prevent HTRB degradation (Fig.6). Additional approach is needed, that is to suppress the value of the critical stress of the specific area inside the Si near the STI, where the high

stress exists. In particular, the high-dose implanted area should be kept away from the highly stressed area close to the STI by modifying the LDMOS layout design. Fig. 9 shows plan and cross-sectional schematic views of (a) conventional and (b) GC-covered structure, which STI/Si-interface is covered by gate poly Si. Modified structure (Fig. 9(b) and (d)) keeps high-dose ion implantation area away from STI/Si-interface. The HTRB result of GC-covered structure with STI filling material-B is shown in Fig. 10. In comparison to the HTRB result of the conventional structure (Fig. 6), in spite of the stress condition is severe for the GC-covered structure, which the HTRB test of conventional structure took place under  $150^\circ C/1000h$ , while new structure was  $175^\circ C/2000h$ , the ratio of  $I_{dss}$  compared to initial  $I_{dss}$  ( $I_{dss}/I_{dss0}$ ) was 45 and  $<1$ . These results demonstrate that the solution came out from the HTRB degradation mechanism (Fig.8), which to keep the high-dose implanted area away from the STI was meaningful to suppress  $I_{dss}$  increase under the HTRB stress. In conclusion, it is necessary to take into account the high dose ion implantation damage as well as STI's mechanical stress due to STI filling material's density at the same time. As a result, competitive low resistance ( $R_{onA} = 1.67m\Omega \cdot mm^2$ ) LDMOS has been successfully fabricated (Fig. 11).

#### Mechanism of leakage current increase under HTRB stress

- (1) Growth of the dislocation due to high-dose implantation near the STI/Si edge
- (2) Treatment of the dislocation by hydrogen ( $H^+$ ) termination to the dangling bonds under the  $N_2/H_2$  anneal
- (3)  $H^+$  de-termination from dangling bonds under the HTRB
- (4) Increase of the leakage current after HTRB stress

\*Wafer baking after HTRB accelerates the  $H^+$  de-termination and increases the leakage current

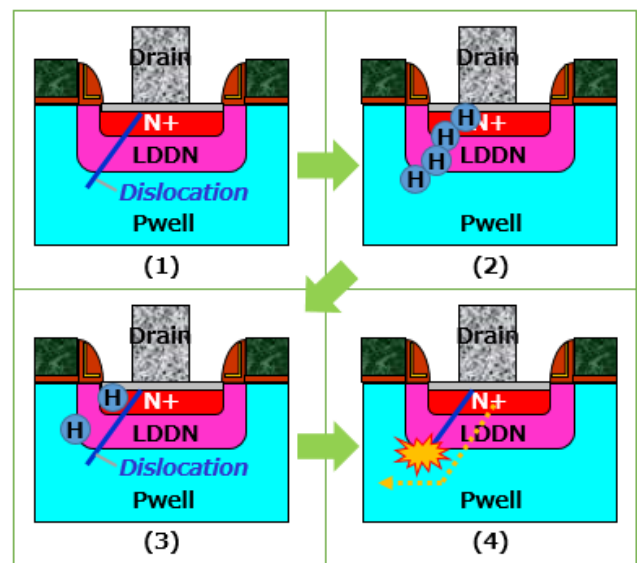


Fig. 8: Explanation of the mechanism of leakage current increase under the HTRB stress.

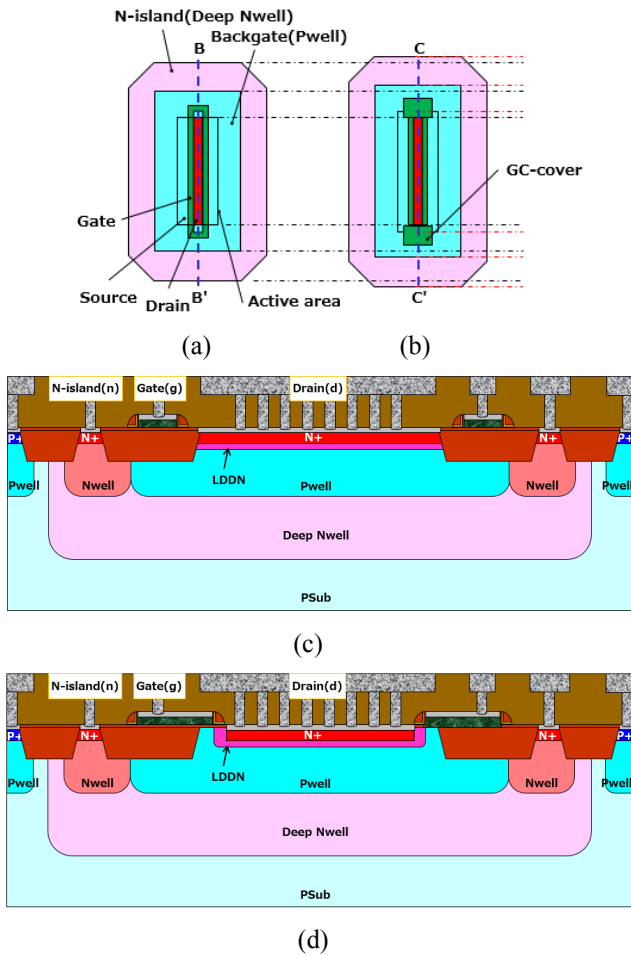


Fig. 9: Plane and cross-sectional views of (a) and (c) conventional and (b) and (d) GC-covered structure.

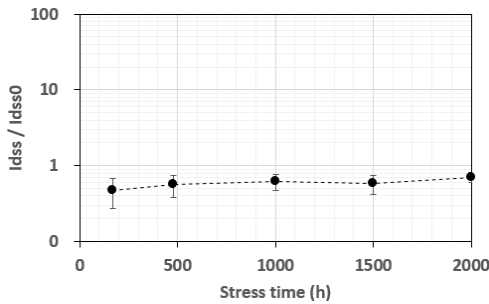


Fig. 10: Measured  $I_{dss}/I_{dss0}$  ( $V_{ds}=8V$ ,  $V_{gs}=0V$ ,  $T=27^{\circ}C$ , 8 points) under the HTRB stress ( $V_{ds}=8V$ ,  $V_{gs}=0V$ ,  $T=175^{\circ}C$ ) of GC-covered structure with STI filling material-B.

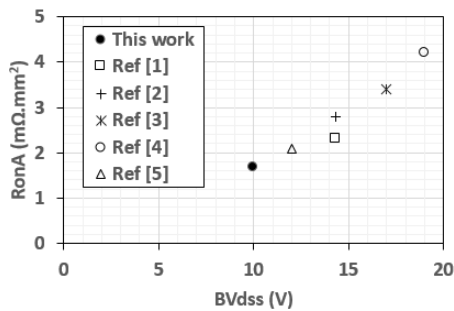


Fig. 11: Comparison of the  $R_{onA}$  vs.  $BV_{dss}$  for NchLDMOS.

## V. CONCLUSIONS

8V NchLDMOS, which has a tolerance against a leakage current ( $I_{dss}$ ) increase and high temperature reverse bias (HTRB) degradation is proposed. Dislocation growth, which results in  $I_{dss}$  increase and has a negative influence on HTRB reliability, occurs because of a high-dose ion implantation and/or mechanical stress due to shallow trench isolation (STI). The studied 8V NchLDMOS was developed by taking into account the mechanism understanding, which to prevent the dislocation growth affecting the device characteristics. As a result, both enough tolerance against HTRB stress and low leakage current with a competitive low resistance ( $R_{onA}=1.67m\Omega \cdot mm^2$ ) has been achieved.

## ACKNOWLEDGMENT

The authors would like to thank Mr. Kenya Kobayashi and Mr. Shinzo Tsuboi for their continuous encouragement and valuable support.

## REFERENCES

- [1] H. L. Chou, P. C. Su1, J. C. W. Ng, P. L. Wang, H. T. Lu, C. J. Lee1, W. J. Syue, S. Y. Yang, Y. C. Tseng, C. C. Cheng, C. W. Yao, R. S. Liou, Y. C. Jong, J. L. Tsai, Jun Cai, H. C. Tuan, Chih-Fang Huang, Jeng Gong, "0.18  $\mu m$  BCD Technology Platform with Best-in-Class 6 V to 70 V Power MOSFETs", Proceeding of the 24<sup>th</sup> ISPSD, pp. 401–404, Jun. 2012.
- [2] R. Roggero, G. Croce, P. Gattari, E. Castellana, A. Molfese, G. Marchesi, L. Atzeni, C. Buran, A. Paleari, G. Ballarin, S. Manzini, F. Alagi and G. Pizzo, "An Advanced 0.16  $\mu m$  Technology Platform with State of the Art Power Devices", Proceeding of the 25<sup>th</sup> ISPSD, pp. 361–364, May 2013.
- [3] F. Jin, D. Liu, J. Xing, X. Yang, J. Yang, W. Qian, W. Yue, P. Wang, M. Qiao and B. Zhang, "Best-in-Class LDMOS with Ultra-Shallow Trench Isolation and P-Buried Layer from 18V to 40V in 0.18 $\mu m$  BCD Technology", Proceeding of the 29<sup>th</sup> ISPSD, pp. 295–298, May 2017.
- [4] L. Wei, C. Chao, U. Singh, R. Jain, L.L. Goh and P.R. Verma, "A Novel Contact Field Plate Application in Drain-Extended-MOSFET Transistors", Proceeding of the 29<sup>th</sup> ISPSD, pp. 335–337, May 2017.
- [5] L. Wei, U. Singh, J. M. Koo, J. Huihua, "A Novel High Performance Medium-Voltage DEnMOS in 40nm CMOS Technology", Proceeding of the 30<sup>th</sup> ISPSD, pp. 292–294, May 2018.
- [6] C. Pacha, B. Martin, K. Arnim, R. Brenderlow, D. Schmitt-Landsiedel, P. Seegebrecht, J. Berthold, and R. Thewes, "Impact of STI-induced stress, inverse narrow width effect, and statistical  $V_{sub}$  TH/ variations on leakage currents in 120 nm CMOS", Proceedings of the 30<sup>th</sup> ESSCIRC, pp. 397–400, Sept. 2004.
- [7] F. W. Saris, J. S. Custer, R. J. Schreutelkamp, R. J. Liefing, R. Wijburg, and H. Wallinga, "Avoiding dislocations in ion-implanted silicon" in Microelectronic Engineering, vol. 19, 1992, pp. 357–362.
- [8] K. Takahashi, K. Komatsu, T. Sakamoto, K. Kimura, and F. Matsuoka, "Hot-Carrier Induced Off-State Leakage Current Increase of LDMOS and Approach to Overcome the Phenomenon", Proceeding of the 30<sup>th</sup> ISPSD, pp. 303–306, May 2018.
- [9] M. H. Park, S. H. Hong, S. J. Hong, T. Park, S. Song, J. H. Park, H. S. Kim, Y. G. Shin, H. K. Kang, and M. Y. Lee, "Stress Minimization in Deep Sub-Micron Full CMOS Devices by Using an Optimized Combination of the Trench Filling CVD Oxides", IEDM Technical Digest, 1997, pp. 669-672.
- [10] C. Lin, Y. Jin, C. H. Jan, C. W. Hu, K. Chang, and H. Kao, "Novel Current Re-Distribution Structure for Improved and Easy-to-Manufacturing 24V LDMOS", Proceeding of the 30<sup>th</sup> ISPSD, pp. 295–298, May 2018.